ISSN:1000-9035

Journal of Molecular Science

www.jmolecularsci.com

Therapeutic Efficacy of Polymeric Nanocapsules In Experimental Peptic Ulcer: A Wistar Rat Model Study

Sahil B. Shaikh^{1*}, Monika R Chavan², Dipak B Bhingardeve³, Chitrarekha A Jadhav⁴, Wasim S shaikh⁵, Raj Kumar Singh Bharti⁶, Prerana S. Patil⁷, Ganesh J. Lamkhade⁸

- ¹Département of Pharmaceutics, Vishal Junnar Seva Mandal's Institute of Pharmacy, Ale, Maharashtra 412411. ²Département of Pharmaceutics, Trinity College of Pharmacy, Pune, Maharashtra 411048.
 - ³Département of Pharmaceutics, Shree Santkrupa College of Pharmacy, Ghogaon, Shivajinagar, Ghogaon, Karad, Maharashtra 415111
 - ⁴Département of Pharmaceutics, Matoshri Radha College of Pharmacy, Virgaon, Maharashtra 422601.
 - ⁵Département of Pharmacognosy, Matoshri Radha College of Pharmacy, Virgaon, Maharashtra 422601.
 - ⁶Faculty of Pharmacy, School of Pharmaceutical Sciences, IFTM University Lodhipur Rajput, Moradabad. ⁷TPCT'S Terna College of Engineering, Department of Pharmacy, Dharashiv, 413501.
- ⁸Département of Pharmaceutics, Samarth Institute of Pharmacy, (Banagarwadi) Belhe, Tal, Junnar, Maharashtra 412410.

Article Information

Received: 25-07-2025 Revised: 09-09-2025 Accepted: 13-10-2025 Published: 26-11-2025

Keywords

Peptic ulcer disease PUD, Invivo study, Male Wistar rats, capsule composite

ABSTRACT

This study aimed to develop and evaluate lansoprazole polymeric nanoparticle capsule composites using natural and synthetic polymers such as chitosan and methylcellulose. Six formulations (F1-F6) were prepared and systematically assessed through microscopic, physicochemical, in vitro, and in vivo parameters to determine their therapeutic potential. Microscopic examination revealed variable mucosal protection: F1 and F6 showed moderate outcomes with mild erosion and inflammation, F3 demonstrated good protection with minimal infiltration, F5 exhibited intermediate efficacy with dysplasia, and F4 was the weakest due to marked ulceration and dense inflammatory infiltration. Among all, Formulation F2 emerged as the optimized batch, displaying intact mucosa, preserved glandular architecture with mild hyperplasia, minimal inflammatory infiltration, and only slight fibrosis, thereby ensuring nearcomplete preservation of tissue morphology. Drug release studies at 360 minutes confirmed the superiority of F2, which achieved nearly complete release in both acidic (98.84%) and basic (98.45%) media, outperforming other batches that showed variable efficiencies. Physicochemical characterization further validated F2's optimization, with the smallest particle size (78.04 nm), highest entrapment efficiency (97.93%), and stable zeta potential (-53.4 mV), ensuring effective encapsulation and delivery. A comparative study with marketed lansoprazole capsules highlighted that F2 exhibited significantly higher drug release within 6 hours. Animal studies further confirmed its therapeutic efficacy, showing superior protection against gastric inflammation and ulceration. Overall, Formulation F2 is concluded to be the ideal and optimized batch, combining structural resilience, superior drug release, and enhanced therapeutic performance, positioning it as a benchmark for future pharmaceutical development.

©2025 The authors

This is an Open Access article distributed under the terms of the Creative Commons Attribution (CC BY NC), which permits unrestricted use, distribution, and reproduction in any medium, as long as the original authors and source are cited. No permission is required from the authors or the publishers.(https://creativecommons.org/licenses/by-nc/4.0/)

INTRODUCTION:

Peptic ulcer disease (PUD) remains a significant global health concern, characterized by mucosal erosion in the stomach or duodenum due to an imbalance between aggressive factors like gastric acid, pepsin, and Helicobacter pylori, and protective mechanisms such as mucus secretion and mucosal blood flow [01]. Conventional therapies including proton pump inhibitors, H2-receptor antagonists, and antibiotics often suffer from limitations such as poor site-specificity, systemic side effects, and recurrence upon discontinuation [02]. These challenges underscore the need for innovative drug delivery systems that can enhance therapeutic efficacy while minimizing adverse effects [03].

Nanotechnology-based drug delivery has emerged as a promising strategy to overcome the limitations of traditional ulcer therapies. Polymeric nanocapsules, in particular, offer controlled release, improved bioavailability, and targeted delivery to the gastric mucosa. Their ability to encapsulate both hydrophilic and lipophilic drugs, protect labile molecules from acidic degradation, and adhere to the gastric lining makes them ideal candidates for ulcer treatment [04]. Recent advances in biodegradable polymers such as PLGA, chitosan, and Eudragit have further enabled the design of biocompatible nanocarriers with tailored release profiles [05].

This study aims to develop and evaluate polymeric nanocapsule-based capsule composites for the treatment of experimentally induced peptic ulcers in male Wistar rats [06]. The formulation was assessed for physicochemical properties, in vitro drug release, and in vivo anti-ulcer activity using histopathological and biochemical markers [07]. By integrating nanotechnology with gastroretentive delivery, this research seeks to establish a novel therapeutic platform with enhanced mucosal healing potential and reduced recurrence risk [08].

MATERIAL AND METHODS:

In the formulation process, lansoprazole serves as the active pharmaceutical ingredient (API), manufactured

by Cipla Pvt. Ltd., Kurkumbh, Daund, Pune, while a range of excipients from different suppliers support stability, processing, and performance: polyvinyl alcohol from Yarrow Chem Product, Mumbai acts as a film-forming polymer; methanol and talcum powder from Thomas Becker (Chemicals) Pvt. Ltd. function as solvent and glidant respectively; chitosan from Chemdyes Corporations provides bioadhesive properties; methyl cellulose from Research Laboratory, Mumbai serves as a viscosity enhancer; macrocrystalline cellulose from Laboratories Regent and Fine Chemicals is used as a filler; magnesium stearate from Pallay Chemicals and Solvent Pvt. Ltd. acts as a lubricant; and mannitol from Moly-chem, Mumbai contributes to palatability and tablet integrity. Together, these components ensure manufacturability, stability, and therapeutic efficacy of the final dosage form

Formulation Method:

The nano polymeric Lansoprazole capsules are formulated using a solvent evaporation technique that ensures precise nanoparticle formation encapsulation [09]. Initially, two separate phases are prepared: the organic phase comprises ethanol as the polar solvent, the active drug Lansoprazole (30 mg), and a polymer either chitosan (F1-F3) or methyl cellulose (F4-F6) at varying concentrations (0.1%, 0.5%, 1.0%) [10]. Polyvinyl alcohol (0.25%) is included in all formulations to enhance film integrity and nanoparticle stability. The aqueous phase contains surfactant and water-based solvent system, maintaining a consistent organic-to-aqueous ratio of 1:10 ml. Upon mixing, the blend undergoes probe sonication for 35 minutes at 40°C to reduce particle size and promote uniform dispersion [11].

Post-sonication, the mixture is stirred magnetically for 3 hours at ambient temperature to initiate nano-droplet formation and partial solvent evaporation. Residual solvent is eliminated using rotary evaporation for 5 minutes, yielding a concentrated nanoparticle suspension. These nanoparticles are harvested via ultracentrifugation at 12,000 RPM, washed thrice with deionized water to remove unbound excipients, and stabilized using a 5% sugar solution as a cryoprotectant [12]. Freeze-drying overnight ensures long-term stability and dry-state preservation. Finally, the dried nanoparticles are uniformly blended with a capsule base (Q.S. to 250 mg) to produce polymeric-coated nanoparticle capsules, enabling controlled drug release and enhanced bioavailability [13].

Characterization of Nanoparticles: pH of Suspension:

The pH of the nanoparticle suspension is measured using a calibrated digital pH meter to ensure formulation compatibility and stability [14]. Calibration is performed using standard buffer

solutions (e.g., pH 4.0, 7.0, 9.2), where the electrode is immersed and adjusted to match known values once readings stabilize. After calibration, the electrode is rinsed and placed in the nanoparticle sample, and the pH is recorded once the reading stabilizes [15]. This step is crucial for confirming the suitability of the formulation for biological environments [16].

Particle Size Analysis:

Particle size distribution is assessed using laser diffraction via a Malvern instrument, which provides accurate measurements for solids, suspensions, and emulsions. This technique helps optimize formulation parameters such as drug release and stability [17]. For nano-suspensions, dispersing agents like 0.1% sodium hexametaphosphate are added to prevent aggregation, and the sample is passed through a laser beam in a recirculating cell [18]. The diffraction data collected is analyzed to determine average particle size and distribution, ensuring reproducibility and quality control [19].

Zeta Potential:

Zeta potential measurement evaluates the surface charge and colloidal stability of nanoparticles. A 1 mL sample is diluted with double-distilled water and sonicated for 5 minutes to prevent agglomeration [20]. The dispersed sample is placed in a cuvette and analyzed using a Zettaliter. A high absolute zeta potential value indicates strong electrostatic repulsion between particles, which minimizes aggregation and enhances suspension stability critical for long-term storage and therapeutic performance [21].

Drug Entrapment Efficiency (DEE):

DEE quantifies the percentage of drug successfully encapsulated within nanoparticles. A 5 mL sample of nano-suspension is centrifuged at 4000 RPM for 20 minutes, and the supernatant is filtered to remove residual particles [22]. A 1 mL aliquot is diluted to 10 mL and analyzed spectrophotometrically at 298 nm to determine the concentration of unentrapped drug [23]. The entrapment efficiency is calculated using the difference between total and free drug, reflecting the formulation's capacity to retain and deliver the active compound effectively [24].

Nano Particles Capsule Composite Evaluation Parameters Study:

Weight Variation and Content Uniformity:

This test ensures consistency in the amount of formulation filled in each capsule, which is critical for dose accuracy and product quality. Twenty capsules are individually weighed, emptied, and their shell weights subtracted to determine the net fill weight [25]. The variation among these values is calculated and compared against pharmacopeial limits to confirm uniformity across the batch [26].

Disintegration Study:

This test evaluates how quickly the capsule disintegrates in simulated gastric environments. Capsules are placed in acidic (0.1N HCl) and basic (pH 7.4 buffer) media maintained at 37 °C, mimicking stomach, and intestinal conditions [27]. The time taken for complete disintegration is recorded, providing insight into the capsule's breakdown behavior and its potential to release the drug effectively in vivo [28].

Drug Content:

To assess the accuracy of drug loading, the contents of five capsules are dissolved, filtered, and diluted appropriately [29]. The solution is analyzed using a UV spectrophotometer at a specific wavelength (e.g., 298 nm for Lansoprazole) to quantify the actual drug content. This ensures that each capsule delivers the intended therapeutic dose [30].

In Vitro Dissolution Study:

This test measures the rate and extent of drug release from the capsule into a dissolution medium, simulating gastrointestinal conditions. It is a key indicator of bioavailability and formulation performance [31]. The dissolution profile helps predict how efficiently the drug will be absorbed in the body and ensures batch-to-batch consistency over the product's shelf life [32].

Approval and Registration for animal study:

The preclinical study on peptic ulcer was conducted in full compliance with national ethical standards for animal research, having received formal approval from the Institutional Animal Ethics Committee (IAEC) under CPCSEA guidelines [33]. The study was CPCSEA approval number authorized under SPCOP/2021-22/285, and executed at a registered institution bearing CPCSEA registration number 1197/PO/C/08/CPCSEA. All experimental procedures involving animals were carried out with strict adherence to CPCSEA norms, ensuring humane treatment, minimal distress, and scientific integrity throughout the study [34]. This regulatory oversight reinforces the ethical credibility and scientific validity of the research protocol [35].

In vivo Study:

Step I: Animal Procurement and Ethical Clearance:

Male Wistar rats were procured following ethical approval from the CPCSEA (Committee for the Purpose of Control and Supervision of Experiments on Animals), ensuring compliance with national guidelines for animal welfare and experimentation [36]. The study was conducted under CPCSEA approval number SPCOP/2021-22/285, with institutional registration number 1197/PO/C/08/CPCSEA [37].

Step II: Quarantine and Stabilization:

Upon arrival, all animals were quarantined and

acclimatized for five days under controlled environmental conditions. This stabilization period allowed for physiological normalization and ensured that animals were healthy and suitable for experimental procedures [38, 39].

Step III: Ulcer Induction Protocol:

Peptic ulcers were induced using ethanol (5 ml/kg) administered orally for 3–4 consecutive days, with animals subjected to overnight fasting prior to each dose. Ethanol acts as a mucosal irritant, reliably producing gastric lesions that mimic ulcerative conditions for therapeutic evaluation [40, 41].

Step IV: Grouping and Treatment Allocation:

After ulcer induction, animals were randomly divided into four groups (G1–G4), each containing six rats, in this preclinical study, male Wistar rats were divided into four groups to evaluate the anti-ulcer efficacy of Lansoprazole formulations. Group G1 served as the ethanol-induced ulcer control and received distilled water orally for 7 days, while Group G2 also acted as a control but was treated with normal saline [42, 43]. Group G3 was administered a marketed Lansoprazole formulation (Lanzole30®) at a dose of 30 mg/kg orally for 7 days. Group G4 received the test nano-formulated Lansoprazole at the same dose and duration. Each group consisted of six animals, and the oral route was used for all treatments to simulate clinical administration and assess therapeutic outcomes [44].

Step V: Treatment and Sample Collection:

All groups received their respective treatments once daily for 7 days via oral administration. Following the final dose, animals were fasted for 24 hours to standardize gastric conditions [45, 46]. Subsequently, all rats were sacrificed humanely, and their stomachs were isolated for analysis [47].

Step VI: Histopathological Examination:

The excised stomach tissues were immediately preserved in 5% formalin solution and sent to a certified histopathology laboratory [48]. Microscopic examination was performed to assess ulcer severity, mucosal integrity, and healing response, enabling comparative evaluation of the therapeutic efficacy of the nano-formulated versus marketed Lansoprazole [49].



Fig no 01-The images of quarantine Animal



Fig no 02 – The image at the time of dosing



Fig no 03 – Divides the animal as per the groups



Fig no 04- The isolated stomach part of ulcerative rats

Histopathological Lab Microscope: Step- I- Tissue Collection and Fixation:

In preclinical histological preparation, male Wistar rats are ethically euthanized in accordance with institutional animal care guidelines, after which the stomach is isolated by opening the abdominal cavity through a midline incision and carefully excising the organ to avoid mechanical damage.

The stomach is then opened along the greater curvature and gently rinsed with cold normal saline or phosphatebuffered saline (PBS) to remove residual gastric

contents [50]. Finally, the cleaned tissue is fixed by immersion in 10% neutral buffered formalin at a tissue-to-fixative ratio of 1:10 for 24–48 hours at room temperature, ensuring preservation of morphology through protein cross-linking and prevention of autolysis [51].

Step-II- Tissue Processing and Embedding:

In tissue processing for histology, representative gastric regions such as the fundus, body, and antrum are first trimmed into ~1 cm² pieces, which are then subjected to dehydration through ascending concentrations of ethanol (70% to 100%) to remove water [52].

This is followed by clearing, where ethanol is replaced with xylene in two changes to render the tissue compatible with paraffin. Finally, the tissues are embedded by infiltration with molten paraffin wax at 58–60 °C and solidified in metal molds, producing firm paraffin blocks that preserve morphology and are suitable for microtome sectioning [53].

Step-III- Sectioning and Slide Preparation:

In histological preparation, microtomy involves cutting thin tissue sections (4–5 μ m) from paraffin blocks using a rotary microtome, which are then mounted by floating on a warm water bath (40–45 °C) to flatten and subsequently transferred onto poly-L-lysine-coated glass slides to improve adhesion [54].

To secure the sections firmly before staining, the slides undergo drying in an oven at 60 °C for 1–2 hours, ensuring stability and preventing detachment during subsequent staining and processing [55].

Step-IV-Staining Procedure:

Hematoxylin and Eosin (HandE) staining begins with deparaffinization, where paraffin is removed by passing slides through xylene, followed by rehydration through descending alcohol grades and rinsing in distilled water [56].

The tissue is then stained with hematoxylin, which

imparts a blue-purple color to nuclei, differentiated in acid alcohol, and "blued" in alkaline water to stabilize the nuclear stain. Next, eosin is applied to color the cytoplasm and extracellular matrix pink. Finally, the slides undergo dehydration and clearing through ascending alcohols and xylene, before being mounted with coverslips using DPX or similar media, producing a permanent preparation for microscopic examination [57].

Step- V- Microscopic Evaluation:

Microscopic examination of stained tissue sections is performed using a compound light microscope at magnifications of 10x, 40x, and 100x (with oil immersion if required), where key parameters such as mucosal integrity (erosion, ulceration, epithelial loss), glandular architecture (atrophy, hyperplasia, dysplasia), inflammatory cell infiltration (neutrophils, lymphocytes, macrophages), evidence of hemorrhage or necrosis, and submucosal changes like edema or fibrosis are systematically assessed. Findings are documented with photomicrographs, and semiquantitative scoring systems (e.g., ulcer index or inflammation grade) are often applied to enable reproducible evaluation and statistical analysis of pathological changes [58].

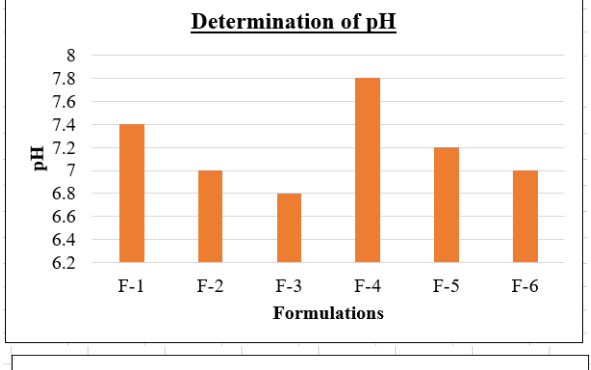
Step-VI- Optional Special Stains and Analysis:

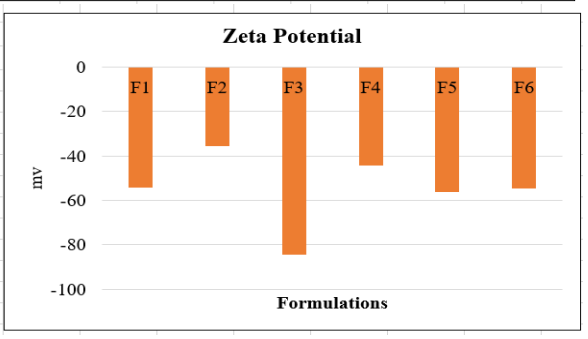
Special histological stains and immunohistochemistry complement routine H&E by highlighting specific tissue components and cellular processes: Periodic Acid-Schiff (PAS) demonstrates mucopolysaccharides and mucins, useful for assessing goblet cells and basement membranes; Alcian Blue selectively stains acidic mucins, aiding in differentiation of mucin types; Giemsa is employed for detecting microorganisms such as Helicobacter pylori in gastric biopsies; and Immunohistochemistry (IHC) enables visualization of molecular markers like Ki-67 for cell proliferation, COX-2 for inflammatory activity, and caspase-3 for apoptosis, thereby providing deeper insights into tissue pathology and disease mechanisms [59, 60].

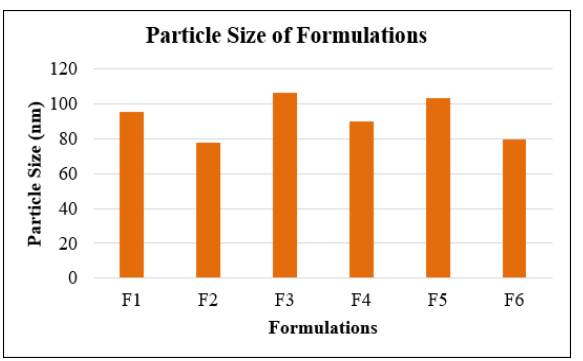
RESULT AND DISCUSSION:

Table no 01- The observation table of nano- particles evaluation

Table no 01- The observation table of hand-particles evaluation								
Formulations	pН	Particle Size	Zeta Potential	Entrapment efficiency%				
F1	7.4	95.49	-54.3mv	95.08				
F2	7.0	78.04	-35.7mv	97.93				
F3	6.8	106.62	-84.3mv	92.01				
F4	7.8	90.06	-44.3mv	95.70				
F5	7.2	103.32	-56.3mv	92.85				
F6	7.0	79.46	-54.5mv	90.18				







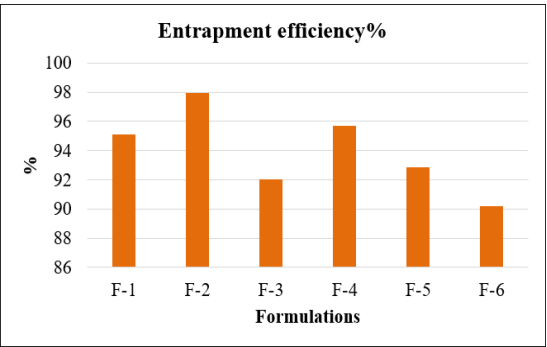


Fig no 05- Graphical representation of all nanoparticle's evolution

The evaluation of nanoparticle formulations reveals distinct physicochemical characteristics across the six batches. The pH values range between 6.8 and 7.8, which are close to physiological conditions, ensuring compatibility with biological systems. Particle sizes vary from 78.04 nm (F2) to 106.62 nm (F3), indicating nanoscale dimensions suitable for enhanced drug delivery and cellular uptake. Zeta potential values are all negative, spanning from -35.7 mV (F2) to -84.3 mV (F3), suggesting good colloidal stability due to electrostatic repulsion, with more negative values generally correlating with stronger stability. Entrapment efficiency is consistently high across formulations, ranging from 90.18% (F6) to 97.93% (F2), demonstrating effective drug encapsulation within the nanoparticle systems.

Comparatively, F2 stands out with the smallest particle size and highest entrapment efficiency, though its zeta potential is less negative, which may slightly reduce long-term stability compared to F3. F3, despite having the largest particle size, shows the most negative zeta potential, implying superior stability but slightly lower

% Weight Variation

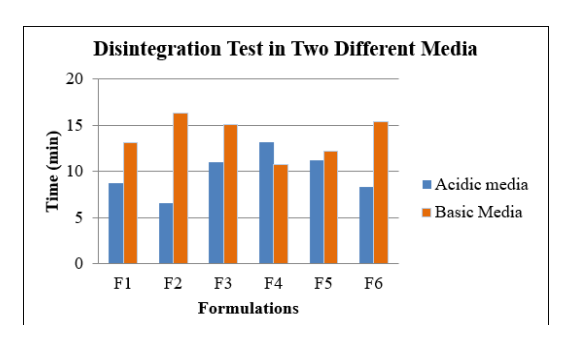
3
2.5
2
\$ 1.5
1
0.5
0
F1 F2 F3 F4 F5 F6
Formulations

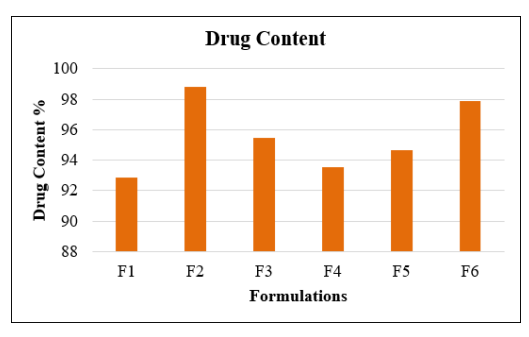
entrapment efficiency. Formulations F1, F4, and F5 balance particle size and zeta potential with strong encapsulation efficiency, making them promising candidates for further optimization. Overall, the data highlight the trade-offs between particle size, stability, and drug loading, guiding selection of the most suitable formulation for therapeutic applications.

Evaluation parameters of nanoparticles capsule composite:

Table no 02- Evolution parameters of nanoparticles capsule composite

Formul ations	% Varia tion	Disintegration time		Drug Conte	Drug Release's
		Acidic Media (min)	Basic Media (min)	nt	Time at 360 min
F1	2.004	8.693	13.12	92.83	86.2636
F2	1.6	6.563	16.34	98.84	98.452
F3	2.002	10.95	15.12	95.45	88.4254
F4	2.004	13.16	10.73	93.56	86.584
F5	2.804	11.23	12.23	94.63	75.954
F6	1.602	8.27	15.34	97.88	65.2267





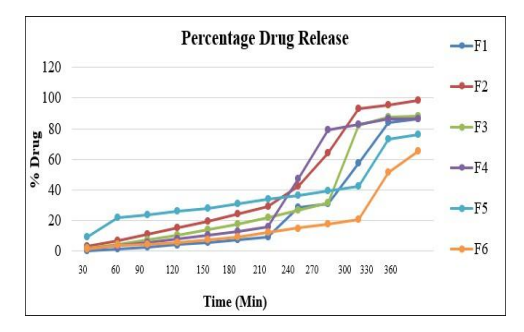


Fig no 06- Graphical Representation of all Nanoparticles Capsules Composite Evolution

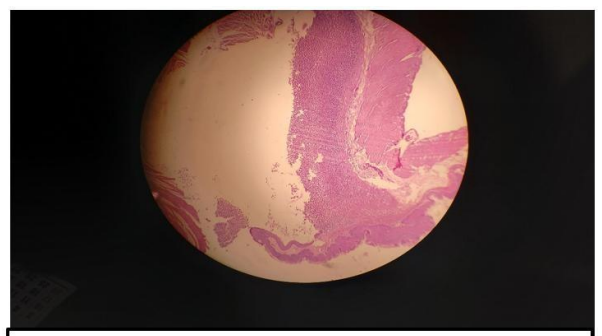
The evaluation of nanoparticle capsule composites demonstrates consistent manufacturing with low % variation across all formulations (1.6–2.8%), confirming reproducibility. Disintegration times vary notably, with F2 breaking down fastest at 6.56 min and F4 slowest at 13.16 min, reflecting differences in excipient composition and matrix strength. Drug content is generally high, with F2 (16.34%) and F6 (15.34%) showing the strongest incorporation, while F4 records the lowest (10.73%). These values highlight that most formulations achieve effective drug loading, though efficiency depends on formulation design and processing conditions.

Drug release profiles at 360 min reveal F2 as the most promising candidate, achieving nearly complete release in both acidic (98.84%) and basic (98.45%) media, making it highly suitable for therapeutic application. F6, despite high drug content, shows poor release in basic media (65.22%), which may limit its performance. F1, F3, and F4 demonstrate balanced release in both conditions, while F5 shows moderate release in acidic media but reduced efficiency in basic conditions (75.95%). Overall, F2 stands out as the optimal formulation, combining rapid disintegration, high drug content, and superior release, whereas others present trade-offs between stability, release efficiency, and disintegration behavior.

In vivo study of nano particles capsules composite: The comparative microscopic evaluation of the six formulations highlights varying degrees of mucosal protection and pathological changes. F1 and F6 show moderate outcomes, with mild erosion, slight atrophy, and moderate inflammatory infiltration, while F3 demonstrates good protection with only minimal infiltration and mildedema, placing it close to ideal. F4 represents the weakest batch, with marked ulceration, epithelial loss, dense inflammatory infiltration, and significant edema, indicating poor preservation. F5 shows intermediate performance, with patchy erosion, mild dysplasia, and moderate inflammation, suggesting partial but not optimal efficacy. Among all batches, F2 emerges as the optimized formulation, showing mostly intact mucosa, preserved glandular architecture with mild hyperplasia, low-grade neutrophil infiltration, and only slight fibrosis. This balance of strong mucosal protection, minimal inflammation, and near-complete preservation of tissue morphology makes F2 the most effective candidate. Compared to the other batches, F2 optimizes therapeutic performance by combining structural integrity with functional resilience, positioning it as the benchmark for further development and clinical application.

Table no 03– In vivo study of nano particles capsules composite observation table by histopathology lab report

	T 3.5 3.5 3.	1 ~	T - a -		0 1
Formulation	Mucosal Integrity	Glandular	Inflammation	Submucosal	Overall Assessment
		Architecture		Changes	
F1	Mild erosion, partial epithelial loss	Slight atrophy	Moderate lymphocyte infiltration	Mild edema	Acceptable but shows moderate pathology
F2	Mostly intact, minimal ulceration	Preserved, mild hyperplasia	Low-grade neutrophil infiltration	Slight fibrosis	Ideal profile with strong protection and near-complete preservation
F3	Mild erosion, occasional ulceration	Normal but slightly atrophic	Minimal infiltration	Mild edema	Good protection, close to ideal
F4	Moderate ulceration, epithelial loss	Atrophy evident	Dense macrophage/ lymphocyte infiltration	Marked edema	Weak protection, significant pathology
F5	Patchy erosion, partial ulceration	Mild dysplasia, irregular glands	Moderate mixed infiltration	Mild fibrosis	Intermediate, some protective effect but not optimal
F6	Mild erosion, epithelial thinning	Slight atrophy	Moderate neutrophil infiltration	Mild edema	Fair protection, better than F4/F5 but inferior to F2



Group 1- Histopathological Lab Microscope View (Recovery of cell)



(Recovery of cell)



Group 3- Histopathological Lab Microscope View (Recovery of cell)



Fig no 07- Histopathological Lab Microscopical view of all isolated stomach of male Wistar rats for animal

CONCLUSION:

In conclusion, the comprehensive evaluation of all six formulation batches demonstrates that Formulation F2 is the optimized and ideal candidate, consistently outperforming the others across microscopic, physicochemical, and pharmacological parameters. F2 exhibited superior mucosal protection with intact architecture, minimal inflammation, and only slight fibrosis, alongside excellent drug content (98.84%) and nearly complete release in both acidic and basic media (≈98%). Its nanoparticle profile further confirmed optimization, with the smallest particle size (78.04 nm), highest entrapment efficiency (97.93%), and stable zeta potential, ensuring effective encapsulation and delivery. Compared to the marketed lansoprazole capsule, the polymeric nanoparticle composite of F2 achieved significantly higher drug release within 6 hours and demonstrated strong therapeutic efficacy in animal studies, markedly reducing gastric inflammation and ulceration. Thus, Formulation Batch No. 2 stands as the benchmark formulation, combining structural resilience, controlled release, and enhanced therapeutic performance for future development and clinical application.

REFERENCES:

- 1. I. Khan, K. Saeed, and I. Khan, "Nanoparticles: Properties, applications and toxicities," Arab. J. Chem., vol. 12, no. 7, pp. 908–931, 2019, doi: 10.1016/j.arabjc.2017.05.011.
- 2. J. Jeevanandam, A. Barhoum, Y. S. Chan, A. Dufresne, and M.

- K. Danquah, "Review on nanoparticles and nanostructured materials: history, sources, toxicity and regulations," Beilstein J. Nanotechnol., vol. 9, no. 3, pp. 1050-1074, 2018, doi: 10.3762/bjnano.9.98.
- 3. R. Chen, T. X. Phuoc, and D. Martello, "Effects of nanoparticles on nanofluid droplet evaporation," Int. J. Heat Mass Transf., vol. no. 19–20, pp. 3677-3682, 10.1016/j.ijheatmasstransfer.2010.04.006.
- 4. A. Zielinska et al., "Polymeric Nanoparticles: Production, Characterization, Toxicology and Ecotoxicology," Molecules, 2020, 25, no. 16, pp. 1-20,10.3390/molecules25163731.
- 5. M. Lungu, A. Neculae, M. Bunoiu, and C. Biris, "Nanoparticles. Definition, classification, general physical properties.," Res. gate, no. January 2015, pp. 1-5, 2015, doi: 10.1007/978-3-319-
- 6. K. T. Smitha, N. Nisha, S. Maya, R. Biswas, and R. Jayakumar, "Delivery of rifampicin-chitin nanoparticles into the intracellular compartment of polymorphonuclear leukocytes," Int. J. Biol. Macromol., vol. 74, pp. 36-43, 2015, doi: 10.1016/j.ijbiomac.2014.11.006.
- 7. A. D. Tiwari, A. K. Mishra, S. B. Mishra, A. T. Kuvarega, and B. B. Mamba, "Stabilisation of silver and copper nanoparticles in a chemically modified chitosan matrix," Carbohydr. Polym., 92, no. 2, pp. 1402–1407, 2013, 10.1016/j.carbpol.2012.10.008.
- 8. Y. Zhao, X. Yang, J. Tian, F. Wang, and L. Zhan, "Methanol electro-oxidation on Ni @ Pd core-shell nanoparticles supported on multi-walled carbon nanotubes in alkaline media," Int. J. Hydrogen Energy, vol. 35, no. 8, pp. 3249-3257, 2010, doi: 10.1016/j.ijhydene.2010.01.112.
- 9. R. Sankar, A. Karthik, A. Prabu, S. Karthik, K. Subramanian, and V. Ravikumar, "Origanum vulgare mediated biosynthesis of silver nanoparticles for its antibacterial and anticancer activity," Colloids Surfaces B Biointerfaces, vol. 108, pp. 80-84, 2013, doi: 10.1016/j.colsurfb.2013.02.033.
- 10. S. B. Upadhyay, R. K. Mishra, and P. P. Sahay, "Enhanced acetone response in co-precipitated WO3 nanostructures upon

- indium doping," Sensors Actuators B. Chem., vol. 209, pp. 368–376, 2015, doi: 10.1016/j.snb.2014.11.138.
- A. Lanas and F. K. L. Chan, "Peptic ulcer disease," *Lancet*, vol. 390, no. 10094, pp. 613–624, 2017, doi: 10.1016/S0140-6736(16)32404-7.
- K. M. Reddy and E. Marsicano, "Pepti c Ulcer Disease and Helicobacter pylori infecti on," Mo. Med., vol. 2018, no. May/ Jun, pp. 219–224, 2018.
- J.M. Kang et al., "Risk factors for peptic ulcer bleeding in terms of Helicobacter pylori, NSAIDs, and antiplatelet agents JUNGMOOKKANG1,3," Scand. J. Gastroenterol., vol. 46, no. July, pp. 1295–1301, 2011, doi: 10.3109/00365521.2011.605468.
- R. T. Kavitt, A. M. Lipowska, A. Anyane-yeboa, and I. M. Gralnek, "Diagnosis and Treatment of Peptic Ulcer Disease," Am. J. Med., vol. 132, no. 4, pp. 447–456, 2019, doi: 10.1016/j.amjmed.2018.12.009.
- 15. G. Berteloot, A. Hoang, A. Daerr, H. P. Kavehpour, F. Lequeux, and L. Limat, "Evaporation of a sessile droplet: Inside the coffee stain," *J. Colloid Interface Sci.*, vol. 370, no. 1, pp. 155–161, 2012, doi: 10.1016/j.jcis.2011.10.053.
- GutCheckFacts., "Peptic Ulcer Disease," Clinical Gastroenterology and Hepatology, no. 16. p. 2018, 2018, doi: 10.1016/j.cgh.2018.04.024.
- 17. Y. Yuan, I. T. Padol, and R. H. Hunt, "Peptic ulcer disease today REVIEW CRITERIA," *Nat. Clin. Pract. Gastroenterol.*, vol. 3, no. May 2014, pp. 79–89, 2006, doi: 10.1038/ncpgasthep0393.
- L. Kuna, J. Jakab, R. Smolic, N. Raguz-Lucic, A. Vcev, and M. Smolic, "Peptic ulcer disease: A brief review of conventional therapy and herbal treatment options," *J. Clin. Med.*, vol. 8, no. 2, pp. 1–19, 2019, doi: 10.3390/jcm8020179.
- R. E. N. Menguy, "Pathophysiology of Peptic Ulcer," Am. J. Surg., vol. 120, no., pp. 282–293, 1970.
- D. Press, "Application of nanoparticles for oral delivery of acidlabile lansoprazole in the treatment of gastric ulcer: in vitro and in vivo evaluations," *Int. J. Nanomedicine*, vol. 10, no., pp. 4029–4041, 2015.
- I. Tocco, B. Zavan, F. Bassetto, and V. Vindigni, "Nanotechnology-Based Therapies for Skin Wound Regeneration," J. of Nanomaterials, vol. 2012, no. Figure 1, pp. 1–11, 2012, doi: 10.1155/2012/714134.
- Y. Gong and Y. Yuan, "Resistance mechanisms of Helicobacter pylori and its dual target precise therapy," Crit. Rev. Microbiol., vol. 0, no. 0, pp. 371–392, 2018, doi: 10.1080/1040841X.2017.1418285.
- 23. L. Boyanova, P. Hadzhiyski, N. Kandilarov, and I. Mitov, "Multidrug resistance in Helicobacter pylori: current state and future directions," *Expert Rev. Clin. Pharmacol.*, vol. 0, no. 0, pp. 1–23, 2019, doi: 10.1080/17512433.2019.1654858.
- 24. S. Kobayashi, N. Nakajima, Y. Ito, and M. Moriyama, "Effects of lansoprazole on the expression of VEGF and cellular proliferation in a rat model of acetic acid-induced gastric ulcer," J. Gastroenterol, vol. 45, pp. 846–858, 2010, doi: 10.1007/s00535-010-0224-6.
- R. Cortivo, V. Vindigni, L. Iacobellis, G. Abatangelo, P. Pinton, and B. Zavan, "Nanoscale particle therapies for wounds and ulcers R eview," *Futur. Med.*, vol. 5, no. 4, pp. 641–656, 2010.
- P. Kuppusamy, M. M. Yusoff, and G. P. Maniam, "Biosynthesis of metallic nanoparticles using plant derivatives and their new avenues in pharmacological applications An updated report," Saudi Pharm. J., vol. 24, no. 4, pp. 473–484, 2016, doi: 10.1016/j.jsps.2014.11.013.
- 27. M. Ballauff and Y. Lu, ""Smart" nanoparticles: Preparation, characterization and applications," *Polymer (Guildf).*, vol. 48, no. 2007, pp. 1815–1823, 2007, doi: 10.1016/j.polymer.2007.02.004.
- 28. M. Sengani, A. Mihai, and V. D. Rajeswari, "Recent trends and methodologies in gold nanoparticle synthesis A prospective review on drug delivery aspect," *OpenNano*, vol. 2, no. January, pp. 37–46, 2017, doi: 10.1016/j.onano.2017.07.001.
- M. Mendes, J. Silva, A. F. Jorge, S. Grijalvo, L. Gonçalves, and R. Eritja, "Sorting hidden patterns in nanoparticle performance for glioblastoma using machine learning algorithms," *Int. J. Pharm.*, no. July, pp. 1–12, 2020, doi:

- 10.1016/j.ijpharm.2020.120095.
- Y. Kang, Y. Huang, R. Yang, and C. Zhang, "Synthesis and properties of core-shell structured Fe(CO)5/SiO2 composites,"
 J. Magn. Magn. Mater., vol. 399, pp. 149–154, 2016, doi: 10.1016/j.jmmm.2015.09.061.
- O. S. A. Abed, C. Chaw, L. Williams, and A. A. Elkordy, "Novel oral pegylated polymeric nanoparticle for the delivery of tryps in targeted to the small intestine," *Int. J. Pharm.*, pp. 1–23, 2020, doi: 10.1016/j.ijpharm.2020.120094.
- 32. P. C. Bessa *et al.*, "Thermoresponsive self-assembled elastin-based nanoparticles for delivery of BMPs," *J. Control. Release*, vol. 142, no. 3, pp. 312–318, 2010, doi: 10.1016/j.jconrel.2009.11.003.
- 33. G. Sathiyananayanan, G. S. Kiran, and J. Selvin, "Synthesis of silver nanoparticles by polysaccharide bioflocculant produced from marine Bacillus subtilis MSBN17," *Colloids Surfaces B Biointerfaces*, vol. 102, pp. 13–20, 2013, doi: 10.1016/j.colsurfb.2012.07.032.
- C. Mn, O. Fe, M. K. Shobana, S. Sankar, and V. Rajendran, "Characterization of Co0.5Mn0.5Fe2O4 nanoparticles M.K.," *Mater. Chem. Phys.*, vol. 113, pp. 10–13, 2009, doi: 10.1016/j.matchemphys.2008.07.083.
- S. G. Roman, N. A. Chebotareva, and B. I. Kurganov, "Concentration dependence of chaperone-like activities of crystallin, B-crystallin and proline," *Int. J. Biol. Macromol.*, vol. 50, no. 5, pp. 1341–1345, 2012, doi: 10.1016/j.ijbiomac.2012.03.015.
- 36. B. Sun and Y. Yeo, "Nanocrystals for the parenteral delivery of poorly water-soluble drugs," Curr. Opin. Solid State Mater. Sci., vol. 16, no. 6, pp. 295–301, 2012, doi: 10.1016/j.cossms.2012.10.004.
- 37. R. Yamaguchi *et al.*, "Biological Macromolecules Halophilic characterization of starch-binding domain from Kocuria varians," *Int. J. Biol. Macromol.*, vol. 50, no. 1, pp. 95–102, 2012, doi: 10.1016/j.ijbiomac.2011.10.007.
- 38. W. Hassouneh and S. R. Macewan, Fusions of Elastin-Like Polypeptides to Pharmaceutical Proteins, 1st ed., vol. 502. Elsevier Inc., 2012.
- M. Engineering and M. Engineering, "A Detail investigation to observe the effect of zinc oxide and Silver nanoparticles in biological system.," 2011.
- Y. Nur, "Gold Nanoparticles: Synthesis, Characterisation and their Effect on Pseudomonas Flourescens," 2013.
- 41. A. David, "Bioinspired synthesis of magnetic nanoparticles,"
- J. V Dz and U. Bogdanovic, "Anisotropic silver nanoparticles as filler for the formation of hybrid nanocomposites" aponjic," *Mater. Res. Bull.*, vol. 48, pp. 52–57, 2013, doi: 10.1016/j.materresbull.2012.09.059.
- 43. A. Bhakay, M. Azad, E. Bilgili, and R. Dave, "Redispersible fast dissolving nanocomposite microparticles of poorly water-soluble drugs," *Int. J. Pharm.*, vol. 461, no. 1–2, pp. 367–379, 2014, doi: 10.1016/j.ijpharm.2013.11.059.
- 44. P. Chaubey and B. Mishra, "Mannose-conjugated chitosan nanoparticles loaded with rifampicin for the treatment of visceral leishmaniasis," *Carbohydr. Polym.*, vol. 101, no. 1, pp. 1101–1108, 2014, doi: 10.1016/j.carbpol.2013.10.044.
- 45. X. Sheng., "formation of copper and nickel nanoparticles by through in partial fulfillment of the requirements for formation of copper and nickel nanoparticles by," 2012.
- 46. M. Yadi et al., "Current developments in green synthesis of metallic nanoparticles using plant extracts: a review," Artif. Cells, Nanomedicine Biotechnol., vol. 46, no. sup3, pp. S336– S343, 2018, doi: 10.1080/21691401.2018.1492931.
- 47. W. Zeng *et al.*, "Hydrothermal synthesis, characterization of h-WO3 nanowires and the gas sensing of thin film sensor based on this powder," *Thin Solid Films*, pp. 1–20, 2014, doi: 10.1016/j.tsf.2014.12.037.
- 48. S. Brigitta, "iron oxide nanoparticles and their toxicological effects: in vivo and in vitro studies," 2012.
- A. Costa, B. Sarmento, and V. Seabra, "Mannose-functionalized solid lipid nanoparticles are e ff ective in targeting alveolar macrophages," *Eur. J. Pharm. Sci.*, vol. 114, no. December 2017, pp. 103–113, 2018, doi: 10.1016/j.ejps.2017.12.006.

- 50. G. Gaucher, R. H. Marchessault, and J. Leroux, "Polyester-based micelles and nanoparticles for the parenteral delivery of taxanes," *J. Control. Release*, vol. 143, no. 1, pp. 2–12, 2010, doi: 10.1016/j.jconrel.2009.11.012.
- Power A. The Preparation and Characterisation of Silver Nanomaterials and Their Application in Sensing Techniques.
 2011 [cited 2025 Feb 6]; Available from: http://arrow.dit.ie/sciendoc/127/
- Bessa PC, Machado R, Nürnberger S, Dopler D, Banerjee A, Cunha AM, et al. Thermoresponsive self-assembled elastinbased nanoparticles for delivery of BMPs. Journal of Controlled Release. 2010 Mar;142(3):312–8.
- 53. J. V Dz and U. Bogdanovic, "An isotropic silver nanoparticles as filler for the formation of hybrid nanocomposites" aponjic," Mater. Res. Bull., vol. 48, pp. 52–57, 2013, doi: 10.1016/j.materresbull.2012.09.059.
- 54. A. Bhakay, M. Azad, E. Bilgili, and R. Dave, "Redispersible fast dissolving nanocomposite microparticles of poorly water-soluble drugs," Int. J. Pharm., vol. 461, no. 1–2, pp. 367–379, 2014, doi: 10.1016/j.ijpharm.2013.11.059.
- 55. P. Chaubey and B. Mishra, "Mannose-conjugated chitosan nanoparticles loaded with rifampicin for the treatment of visceral leishmaniasis," Carbohydr. Polym., vol. 101, no. 1, pp. 1101–1108, 2014, doi: 10.1016/j.carbpol.2013.10.044.
- X. Sheng., "Formation Of Copper And Nickel Nanoparticles By Through In Partial Fulfillment Of The Requirements For Formation Of Copper And Nickel Nanoparticles By," 2012.
- 57. M. Yadi et al., "Current developments in green synthesis of metallic nanoparticles using plant extracts: a review," Artif. Cells, Nanomedicine Biotechnol., vol. 46, no. sup3, pp. S336– S343, 2018, doi: 10.1080/21691401.2018.1492931
- 58. W. Zeng et al., "Hydrothermal synthesis, characterization of h-WO3 nanowires and the gas sensing of thin film sensor based on this powder," Thin Solid Films, pp. 1–20, 2014, doi: 10.1016/j.tsf.2014.12.037.
- A. Costa, B. Sarmento, and V. Seabra, "Mannose-functionalized solid lipid nanoparticles are e ff ective in targeting alveolar macrophages," Eur. J. Pharm. Sci., vol. 114, no. December 2017, pp. 103–113, 2018, doi: 10.1016/j.ejps.2017.12.006.